HHS Public Access

Author manuscript

Epilepsy Res. Author manuscript; available in PMC 2021 May 01.

Published in final edited form as:

Epilepsy Res. 2020 May ; 162: 106320. doi:10.1016/j.eplepsyres.2020.106320.

Characterization and treatment of spontaneous recurrent seizures following nerve agent-induced status epilepticus in mice

Hilary S. McCarren[a], **Margaret R. Eisen**[a], **Dominique L. Nguyen**[a], **Parker B. Dubée**[a], **Cherish E. Ardinger**[a], **Emily N. Dunn**[a], **Kari M. Haines**[a], **Antonia N. Santoro**[a], **Paige M. Bodner**[a], **Celinia A. Ondeck**[a], **Cary L. Honnold**[a], **John H. McDonough**[a], **Phillip H. Beske**[a], **Patrick M. McNutt**[a]

[a]United States Army Medical Research Institute of Chemical Defense, 8350 Ricketts Point Rd Aberdeen Proving Ground, MD 21010, United States of America

Abstract

Purpose: To develop and characterize a mouse model of spontaneous recurrent seizures following nerve agent-induced status epilepticus (SE) and test the efficacy of existing antiepileptic drugs.

Methods: SE was induced in telemeterized male C57Bl6/J mice by soman exposure, and electroencephalographic activity was recorded for 4–6 weeks. Mice were treated with antiepileptic drugs (levetiracetam, valproic acid, phenobarbital) or corresponding vehicles for 14 d after exposure, followed by 14 d of drug washout. Survival, body weight, seizure characteristics, and histopathology were used to characterize the acute and chronic effects of nerve agent exposure and to evaluate the efficacy of treatments in mitigating or preventing neurological effects.

Results: Spontaneous recurrent seizures manifested in all survivors, but the number and frequency of seizures varied considerably among mice. In untreated mice, seizures became longer over time. Moderate to severe histopathology was observed in the amygdala, piriform cortex, and CA1. Levetiracetam provided modest improvements in neurological parameters such as reduced spike rate and improved histopathology scores, whereas valproic acid and phenobarbital were largely ineffective.

Corresponding author: Hilary McCarren, 8350 Ricketts Point Rd, Aberdeen Proving Ground, MD 21010, United States of America, *phone* +1 (410) 436-4287, *fax* +1 (410) 436-2690, hilary.s.mccarren.civ@mail.mil.

Publisher's Disclaimer: Disclaimers

The views expressed in this manuscript are those of the authors and do not reflect the official policy of the CCRP, NIAID, NIH, HHS, USAMRICD Department of Army, Department of Defense, or the U.S. Government. The experimental protocol was approved by the Animal Care and Use Committee at the United States Army Medical Research Institute of Chemical Defense, and all procedures were conducted in accordance with the principles stated in the *Guide for the Care and Use of Laboratory Animals*, the Public Health Service Policy on Humane Care and Use of Laboratory Animals, and the Animal Welfare Act of 1966 (P.L. 89–544), as amended.

Disclosure

Declarations of interest: none.

Conclusions: This model of post-SE spontaneous recurrent seizures differs from other experimental models in the brief latency to seizure development, the occurrence of seizures in 100% of exposed animals, and the lack of damage to CA4/dentate gyrus. It may serve as a useful tool for rapidly and efficiently screening novel therapies that would be effective against severe epilepsy cases.

Keywords

soman; spontaneous recurrent seizures; levetiracetam; valproic acid; phenobarbital; refractory

1. Introduction

Nerve agents are highly toxic chemical weapons that have been employed in warfare, terrorism, and assassination attempts. Thousands of people have been poisoned by nerve agents, including civilians, military members, first-responders, and medical personnel caring for casualties (Office of the Surgeon General, 2008; United Nations Mission to Investigate Allegations of the Use of Chemical Weapons in the Syrian Arab Republic, December 13, 2013; United Nations Security Council, March 26, 1984; Yanagisawa et al., 2006). Recent attacks in Syria, Malaysia, and England have underscored the threat that these chemical weapons pose to modern society. Nerve agents covalently bind and inhibit acetylcholinesterase, which leads to excessive stimulation of muscarinic and nicotinic cholinergic receptors throughout the body. Within the central nervous system, this cholinergic crisis induces a cascade of excitatory neurotransmission that manifests as status epilepticus (SE) (McDonough and Shih, 1997). Like SE of any etiology, nerve agent-induced SE is a medical emergency that can result in long-term neurological deficits. Survivors of nerve agent poisoning have been reported to suffer from retrograde amnesia, impaired cognitive processing, and electrographic epileptiform activity that persists for years after exposure (Office of the Surgeon General, 2008; Yanagisawa et al., 2006). Animal models also suggest that spontaneous recurrent seizures (SRS), which are a defining feature of acquired epilepsy, are a likely consequence of nerve agent-induced SE (de Araujo Furtado et al., 2010; Marrero-Rosado et al., 2018; McDonough et al., 1998; McDonough et al., 1986). While substantial effort has gone towards improving treatments for acute central nervous system (CNS) effects of nerve agents, there is very little preclinical data to guide chronic care.

Epilepsy can be caused by a variety of genetic conditions and traumatic insults. A substantial number of epileptic individuals have to try multiple antiepileptic drugs (AEDs) before they find an effective treatment regimen, and more than one-third of patients never achieve full seizure control (Chen et al., 2018). The difficulty of predicting which AEDs will work for an individual patient is likely due to the underlying heterogeneity of the disease. Because nerve agents act by a well-defined mechanism and cause predictable structural and molecular changes in the brain (Baze, 1993; McDonough et al., 1998; McDonough and Shih, 1997; Shih and McDonough, 1997), certain AEDs may be more appropriate for treating nerve agent-induced epilepsy than others. With approximately 30 AEDs approved by the FDA (Vossler, 2018), an effective therapy or class of therapies could already exist. A rat model of nerve agent-induced SRS has been described (de Araujo Furtado et al., 2010),

and preliminary characterization of nerve agent-induced SRS in mice that lack serum carboxylesterase has also been performed (Marrero-Rosado et al., 2018). However, neither model has yet been used to evaluate the efficacy of currently available AEDs. We chose to develop a C57Bl6/J mouse model of nerve agent-induced SRS as a cost-effective model for screening AEDs in a chronic dosing paradigm. Here we describe disease progression in this exposure model and evaluate the effects of 14 d of treatment with levetiracetam (LEV), valproic acid (VPA), or phenobarbital (PHB) on neuropathology, physiological parameters and seizure burden.

2. Materials & Methods

2.1 Animals:

The experimental protocol was approved by the Institutional Animal Care and Use Committee at the United States Army Medical Research Institute of Chemical Defense, and all procedures were conducted in accordance with the principles stated in the *Guide for the Care and Use of Laboratory Animals*, the Public Health Service Policy on Humane Care and Use of Laboratory Animals, and the Animal Welfare Act of 1966 (P.L. 89–544), as amended. A total of 127 male C57Bl6/J mice (Jackson Laboratory, Bar Harbor, ME), age 12–13 wks at nerve agent exposure, were used for this study. Mice were singly housed in polycarbonate cages with corncob bedding to prevent damage to telemetry implants. A standard 12:12 light dark cycle was used, with lights on at 0600. Food and water were provided *ad libitum*. After nerve agent exposure, additional diet gel and wet mash were provided daily, along with 0.5 mL of subcutaneous (SC) lactated Ringer's solution as needed to promote survival. A subset of animals were removed from the study based on humane endpoint criteria and were euthanized with >200 mg/kg pentobarbital-based euthanasia solution injected intraperitoneally (IP) followed by cervical dislocation. The criteria for humane endpoint removal was simultaneous observation of two or more of the following characteristics at greater than 24 h after onset of SE: moderate to marked abdominal breathing, greater than 30% reduction in body weight compared to baseline, extreme lethargy, and unresponsiveness to external stimuli. For the purposes of survival calculations, these animals were considered to have died on the day they were euthanized.

2.2 Surgery:

All mice were implanted with ETA-F10 telemetry transmitters (Data Sciences International; DSI) at Jackson Laboratory for chronic electrographic recordings. Mice were anesthetized with 400 mg/kg tribromoethanol (IP), and biopotential leads were placed bilaterally over the parietal cortex, approximately 2 mm posterior and 1.5 mm lateral to bregma. Analgesia was provided in the form of 5 mg/kg carprofen (SC) and topical administration of 0.1% solution of bupivacaine. Mice were allowed to recover and acclimate for 3 wk prior to nerve agent exposure.

2.3 Nerve Agent Exposure:

Exposures were conducted on groups of up to 16 mice at a time. Baseline electroencephalographic (EEG) activity was collected in the mouse's home cage for 24 h prior to nerve agent exposure. On the morning of exposure, mice were administered 50

mg/kg HI-6 dimesylate (10 mg/ml in saline, IP) at 5 min prior to nerve agent challenge. Soman (172 μg/kg, 60 μg/ml in saline, SC) was then administered in the mouse's flank. After 1 min, mice were given 2 mg/kg atropine methyl nitrate (AMN, 0.5 mg/ml in saline, IP). HI-6 and AMN were used to mitigate the acute mortality associated with peripheral toxicity of nerve agent so that chronic CNS symptomology could be observed. Electrographic SE onset was determined as previously described (McCarren et al., 2018), and occurred an average of 16.2 ± 12.1 min after soman exposure. Diazepam (5 mg/kg, 1 mg/ml in saline, IP) was administered to each mouse at 2 h after SE onset. The timing and doses of soman, AMN, and diazepam were chosen based on pilot studies that aimed to optimize the exposure paradigm for high survival, convulsion rate, and histopathological damage severity.

2.4 AED treatment:

Saline (SAL, 4 ml/kg) was used as the vehicle control for LEV and VPA. LEV was prepared at 25 mg/ml in SAL and dosed at 100 mg/kg. VPA was prepared at 50 mg/ml in SAL and dosed at 200 mg/kg. The vehicle control for PHB (PHB VEH, 2 ml/kg) was comprised of 3.1% propylene glycol, 3.7% distilled water, 0.8% ethanol, and 0.12% benzyl alcohol in SAL. PHB was prepared at 10 mg/ml in PHB VEH and dosed at 20 mg/kg. Treatment with AEDs or corresponding vehicles started 20–22 h after nerve agent exposure and continued for 14 d. LEV, VPA, and SAL were administered IP every 8 h. PHB and PHB VEH were administered SC every 12 h. The doses and dosing schedules for AEDs were chosen based on published rodent data demonstrating sustained drug serum levels that are considered therapeutic in humans (Leite and Cavalheiro, 1995; Loscher and Honack, 2000; Patsalos et al., 2008). All AEDs and vehicles were followed by a 14 d washout period with no treatment.

Assignment of mice to AED treatment groups was performed prior to the start of each nerve agent exposure, with the goal of obtaining 11 mice per group that survived until the end of the study. This number was chosen based on a sample size calculation that assumed 80% power to detect a similar effect to that observed by Leite, et al. (Leite and Cavalheiro, 1995). Mortality that had occurred during previous exposures was taken into account (i.e. groups with higher mortality rates had more animals assigned to them). Up to two AEDs were tested during each experimental cohort to minimize the likelihood of drug dosing errors.

2.5 Histopathology:

At either 43 d (for model characterization mice) or 29 d (for mice treated with AEDs/vehicles) after nerve agent exposure, mice were deeply anesthetized with 75–100 mg/kg IP pentobarbital-based solution and euthanized by exsanguination with 50 mL of phosphate buffered saline followed by 50 mL of 4% paraformaldehyde. Brains were extracted, post-fixed in 4% paraformaldehyde at 4° C for at least 24 h, and paraffin embedded, and sections were cut at 5–10 μm. The coronal section corresponding to 2.06 mm posterior to bregma was stained with hematoxylin and eosin (H&E) per conventional histological methods. A treatment-blinded, board-certified veterinary pathologist scored each of the regions of interest (piriform cortex, amygdala, CA1, CA2/3, and CA4/dentate gyrus [DG]) using the 5-

point scale shown in Figure 1C, where scores are assigned based on the percentage of the region displaying neuronal loss or necrosis.

2.6 EEG Recording and Analysis:

EEG recordings were conducted in the animal's home cage using DSI RPC-1 or RSC-1 receivers connected to Matrix 2.0 data exchange matrices. Data were collected with Ponemah v5.2 or v6.3 at a sampling rate of 500 Hz. A digital 1 Hz high-pass filter was applied to the data. Custom automated analysis was developed using NeuroScore v3.2 and verified against manual scoring for mice in the model characterization portion of the study. The parameters used to identify SRS were: absolute spike amplitude of 200 – 400 μV, individual spike duration of 1–20 ms, spike frequency of 4–50 Hz, spike train duration of at least 10 seconds, and a train join interval of 60 s (i.e., two or more SRS were considered to be a single event if they occurred within 60 s of each other). Data from 0–48 h following soman exposure were excluded from SRS analysis because mice remained in SE throughout the majority of this time period.

2.7 Statistics:

All data were graphed and analyzed using GraphPad Prism v7.04. Where appropriate, data were tested for normality with the D'Agostino & Pearson test and analyzed using parametric or nonparametric methods based on these outcomes. Latencies to onset of convulsions and onset of electrographic SE were compared in the model characterization portion of the study using the Wilcoxon matched-pairs signed rank test. Changes in body weights for each animal were calculated relative to their own baseline weight. A group's weight was considered to have returned to baseline on the first day that the relative group mean did not differ from 100% based on a one-sample t-test. Survival curves for animals treated with AEDs were compared to those from the corresponding vehicle group using the log-rank test. Changes in average daily SRS duration and spike rate over time were considered significant if the slope of the best-fit line was significantly non-zero based on F tests. For AED-treated animals, latency to first SRS was compared to the corresponding vehicle group with an unpaired t-test (LEV and PHB) or a Mann-Whitney test (VPA). The total numbers of SRS during the treatment and washout phases for each AED and related vehicle were compared using repeated measures two-way ANOVAs. The best-fit lines for SRS duration and spike rate during treatment and washout were compared between AEDs and vehicles using ANCOVAs to compare slopes and intercepts. Histopathology scores for animals treated with LEV, VPA, and PHB were compared to those from appropriate control animals using Mann-Whitney tests for each brain region. A Bonferroni adjustment was made to control the experiment-wise error (false positive rate) when the saline control group was used for separate comparisons to LEV and VPA. Data are presented as mean ± SD unless otherwise described.

3. Results

3.1 Model Characterization:

A total of 20 mice were exposed to soman and not treated with vehicle or AEDs to establish the soman exposure model, with 11 surviving through 43 d. Of the 9 spontaneous deaths and

humane endpoints, 78% occurred within 96 h after soman exposure (Figure 1A). Among those that survived to 43 d, average body weight returned to pre-exposure baseline by 2 d post-exposure (101.9% ± 4.5% of baseline weight), but did not begin to steadily increase pre-exposure baseline by until 14 d post-exposure (Figure 1B). Histopathologic lesions were observed in 83% of survivors (Figure 1C), with the most severe damage consistently observed in the CA1 region of the hippocampus, the amygdala, and the piriform cortex (Figure 1D–F). No damage was observed in CA4/DG in any mice.

Following soman exposure, the latency to onset of convulsions was significantly shorter than the latency to electrographic SE ($p < 0.0001$, median difference = 326.5 s, $n = 18$), illustrating the importance of EEG recordings for accurately identifying and characterizing seizure activity. SRS events were observed in 100% of surviving mice ($n = 10$; one mouse was excluded because of poor EEG signal). SRS events had a characteristic shape, initiating with high-frequency spikes of increasing amplitude, which transitioned to a waveform dominated by low-frequency activity followed by a brief period of post-ictal suppression (Figure 2A–B). Mice exhibited robust inter-animal variability in latency to first SRS (median: 2 d, range: 2–14 d), total number of SRS events (median: 56 events, range: 17–161 events), and SRS frequency (median: 1 event/d, range: 0–23 event/d; Figure 2C). Over the course of the study, the average SRS event duration increased for 70% of mice (Figure 2D). Average spike rate during SRS events remained constant for 80% of mice, whereas one mouse showed a significant increase in spike rate over time and another showed a significant decrease (Figure 2E).

3.2 Evaluation of AEDs:

Of 107 soman-exposed mice, 29.9% died prior to the first administration of AED or vehicle. The remaining mice were distributed among treatment groups as follows: 15 (LEV), 13 (SAL), 14 (VPA), 21 (PHB), and 12 (PHB VEH). Survival curves for LEV, VPA, and PHB did not differ from vehicle controls ($p = 0.88$, $p = 0.88$, and $p = 0.65$ respectively; Figure 3A–C). The final numbers of surviving mice for each treatment group that were included in SRS and histopathology analysis were 12 (LEV), 9 (SAL), 11 (VPA), 10 (PHB), and 9 (PHB VEH). Recovery of body weights among the LEV, PHB, and SAL treatment groups was similar to that of the untreated controls in the model characterization study, with the first non-significant difference from baseline occurring at 2 d for LEV and PHB and 4 d for SAL. The remaining treatment groups demonstrated delayed recovery, with body weight returning to baseline at 15 d for VPA and 6 d for PHB VEH (Figure 3D–F). Attempts to withdraw dietary and fluid supplements on the 15th study day resulted in a decline in mean body weight for all groups except LEV, so these supplements were restored to all mice for the remainder of the study.

Similar to untreated mice, those treated with an AED or vehicle exhibited wide variability in latency to first SRS event (Figure 4A) and total number of SRS events throughout the study (Figure 4B). The latency to first SRS event for animals treated with LEV (6.8 ± 4.1 d) or VPA (8.2 ± 7.4 d) did not differ from that of animals treated with the corresponding vehicle SAL (7.5 ± 4.6 d; $p = 0.72$ and 0.90, respectively). In contrast, PHB treatment delayed onset of first SRS event compared to PHB VEH (9.3 ± 3.9 versus 5.0 ± 3.8 d; $p = 0.019$). The total

number of SRS events in the LEV and SAL groups was not significantly affected by treatment ($p = 0.18$) or washout ($p = 0.82$), and no interaction was apparent between the two variables ($p = 0.55$). Similarly, comparison between VPA and SAL treatment revealed no effect of drug ($p = 0.34$), washout ($p = 0.062$), or variable interaction ($p = 0.35$) on total number of SRS events. Treatment with PHB or PHB VEH had no effect on total number of SRS events ($p = 0.18$), and there was no effect of washout ($p = 0.37$) or interaction between the two variables ($p = 0.43$). For all comparisons, the most significant source of variation was differences between subjects, which accounted for 77.9% (LEV vs. SAL), 62.3% (VPA vs. SAL), and 67.9% (PHB vs. PHB VEH) of total variation.

The average SRS duration and spike rate for each treatment group during the treatment and washout phases did not differ between AED-treated groups and controls (Figure 4C–H), with several notable exceptions. The best-fit lines for duration of SRS in LEV-treated animals and VPA-treated animals during the washout period had significantly lower intercepts than in SAL-treated controls ($p = 0.021$ and $p < 0.0001$ respectively, Figures 4C–D), suggesting that both drugs prevented or delayed the progressive lengthening of seizures that was observed during model characterization. Additionally, the best-fit line for the average spike rate among LEV-treated animals had a lower intercept than controls during both the treatment phase ($p < 0.0001$) and washout phase ($p < 0.0001$; Figure 4F), suggesting that LEV causes reduced spike rates during treatment that are maintained after the drug is withdrawn.

Histopathology scores from AED- and vehicle-treated mice were consistent with those of untreated controls, with the most neurotoxicity manifesting in the piriform cortex, the amygdala, and CA1 (Figure 5). Compared to SAL controls, LEV-treated mice had significantly lower histopathology scores in the amygdala ($p < 0.0001$), CA1 ($p = 0.008$), and CA4/DG ($p = 0.026$), but not in the piriform cortex or CA2/3. There were no significant differences between the VPA and SAL groups, nor the PHB and PHB VEH groups, in any brain region.

4. Discussion

The model of soman-induced epilepsy described in this manuscript is unique in the emergence of SRS in 100% of subjects. The consistent and rapid onset of SRS following soman-induced SE offers a practical advantage over other rodent chemoconvulsant epilepsy models that exhibit long latent periods and variable SRS incidence, such as pilocarpine or systemic kainic acid administration. However, the utility of the soman model comes at the cost of 30–40% acute mortality within the first 96 h after intoxication. In comparison, the existing rat model of soman-induced SRS takes a more conservative approach, with lower acute mortality but an SRS development rate of only 29% (de Araujo Furtado et al., 2010). This suggests that, despite its extreme toxicity, soman may be titratable as an epilepsy induction agent. Further optimization of either the mouse model described herein or the lower-dose soman rat model could help to capitalize on the benefits that both provide. The choice to use C57Bl6/J mice in this study was based upon the widespread utilization of this strain throughout the research community, but recent data suggest that this strain is an outlier in terms of its red blood cell acetylcholinesterase activity and toxicity response to sarin

(Matson et al., 2018). One way to improve survivability of the soman mouse model may be to use BALB/c or FVB mice, which are more resistant to the lethal effects of organophosphate compounds than are a variety of other strains (Clement et al., 1981; Matson et al., 2018; Wehner et al., 1987).

All cohorts of mice exhibited moderate to severe histopathologic lesions in the amygdala, piriform, and CA1 region of the hippocampus. This is consistent with other models of post-SE-induced SRS (Brandt et al., 2003; Siso et al., 2017; Turski et al., 1984), except for the lack of damage to the CA4/DG. Cell loss within the DG is believed to lead to synaptic reorganization and subsequent aberrant firing within the hippocampal circuit, which is thought to be a primary cause of SRS (Dudek et al., 1994; Sloviter, 1987; Tauck and Nadler, 1985). However, there is also substantial evidence to suggest that this process is not necessary for SRS to emerge (Brandt et al., 2004; Elmer et al., 1997; Harvey and Sloviter, 2005; Longo and Mello, 1998), as appears to be the case in this model. In general, there is considerable variability in histopathological signatures across animal models of SRS, likely due to species and/or strain differences as well as minor variations in experimental protocols (Ben-Ari and Dudek, 2010). The translational and functional significance of these differences, and how they change responses to AEDs, requires further exploration (Klein et al., 2018; Sloviter, 2009).

Interestingly, two animals in the model characterization phase of this study demonstrated electrographic SRS but did not have appreciable histopathological lesions in any of the regions examined. This contrasts with the long-held doctrine that SE causes excitotoxic brain damage that leads to development of SRS. One interpretation is that the events labeled SRS in this study are not truly spontaneous, but rather a long-lasting and ongoing consequence of the primary nerve agent exposure. This interpretation is further supported by the absence of a latent period in a number of animals, though others have reported the presence of recurrent seizures within 3–4 d of SE (Bumanglag and Sloviter, 2008; Jung et al., 2007; Marrero-Rosado et al., 2018). Ultimately, whether or not the seizures in this study were truly spontaneous is of little relevance since there is good evidence that epileptic maturation is a progressive process rather than a rapid deterioration of healthy brain activity that occurs entirely before the first epileptic seizure (Sloviter, 2008; Williams et al., 2009). The two animals in which pathological lesions were not observed also had fewer seizures than all but one other animal in the study (5th and 7th rows from the top in Figure 2C). It is possible that the SRS events themselves contributed to the development of histopathology in the regions examined, either alone or in combination with the primary SE insult. If SRS events are important contributors to brain damage following nerve agent exposures, then therapeutic interventions at post-acute time points are imperative for recovery.

Similar to other post-SE SRS models, we observed a high degree of inter- and intra-animal variability in SRS occurrence in both untreated and AED-treated animals (de Araujo Furtado et al., 2010; Grabenstatter et al., 2005; Gu and Dalton, 2017; Lemos and Cavalheiro, 1995). The resulting sparsity and clustering of SRS events is a common challenge in preclinical epilepsy research that complicates assessment of treatment efficacy. One way in which this study attempted to combat this issue was by using a treatment-washout crossover design to increase statistical power. Other approaches, such as selecting mice with the greatest

numbers of seizures for treatment, were less feasible due to the difficulty of maintaining animal body weight and general condition over a sufficient period of time to sort animals based on seizure burden. This challenge may have been related to the stress of daily handling and repeated injections, which could be overcome by administering AEDs through chow or programmable mini-pumps. Interestingly, we did not observe any relationship between handling of animals and induction of seizures, which avoids an inconvenient confound that is present in some other models (Loscher, 2007).

Among the three AEDs tested, only LEV showed an appreciable disease modifying effect, as evidenced by reduced spike rate during SRS, blockade of the increase in SRS duration seen in model characterization animals, and reduced histopathology scores in several brain regions relative to controls. These effects were consistent with other reports of modest alterations in seizure severity and pathology in LEV-treated animals (Doheny et al., 2002; Itoh et al., 2015; Kim et al., 2010; Klitgaard et al., 1998; Loscher and Honack, 2000). There was no evidence in this study of tolerance to LEV, which others have reported (Loscher and Honack, 2000; van Vliet et al., 2008). Rather, the positive effects of LEV seemed to extend into the washout period, which argues that even short periods of treatment with LEV may permanently disrupt disease progression, possibly through its neuroprotective properties (Deshpande and DeLorenzo, 2019; Itoh et al., 2015). PHB, on the other hand, delayed the emergence of SRS relative to controls, but had no effects on total seizure burden, severity, or neuropathology. This is consistent with acquired resistance to PHB, which is a well-known characteristic of this drug. VPA was ineffective at altering any seizure or histopathology metric, despite its success in other post-SE animal models (Brandt et al., 2006; Leite and Cavalheiro, 1995; Turski et al., 1987; van Vliet et al., 2010).

It is important to note that a single dose of each AED was tested in this study. Though selected doses were on the high end of what has been reported to be effective, available dose-response data are predominantly from rats rather than mice. Dosing schedules were also chosen based upon published pharmacokinetic data from rats (Leite and Cavalheiro, 1995; Loscher and Honack, 2000), and plasma AED levels were not confirmed. It is possible that alternative dosing strategies could have improved seizure control. However, the lack of efficacy of three drugs with diverse mechanisms of actions suggests that this model of SRS may be resistant to treatments that generally work in other models. It could be an excellent platform to rapidly evaluate novel therapies that might offer hope in the most severe epilepsy cases.

Acknowledgements

The research described was supported by an interagency agreement (AOD16024-001-01000) between the NIH Office of the Director (OD) and the U.S. Army Medical Research Institute of Chemical Defense under the oversight of the Chemical Countermeasures Research Program (CCRP) within the Office of Biodefense Research (OBRS) at the National Institute of Allergy and Infectious Diseases (NIAID/NIH). Support was provided through appointments to the Postgraduate Research Participation Program at the U.S. Army Medical Research Institute of Chemical Defense administered by the Oak Ridge Institute of Science and Education through an interagency agreement between the U.S. Department of Energy and the U.S. Army Medical Research and Development Command.

References

Baze WB, 1993 Soman-induced morphological changes: an overview in the non-human primate. Journal of Applied Toxicology 13, 173–177. [PubMed: 8326086]

Ben-Ari Y, Dudek FE, 2010 Primary and secondary mechanisms of epileptogenesis in the temporal lobe: there is a before and an after. Epilepsy Currents 10, 118–125. [PubMed: 20944823]

Brandt C, Ebert U, Loscher W, 2004 Epilepsy induced by extended amygdala-kindling in rats: lack of clear association between development of spontaneous seizures and neuronal damage. Epilepsy Research 62, 135–156. [PubMed: 15579302]

Brandt C, Gastens AM, Sun M, Hausknecht M, Loscher W, 2006 Treatment with valproate after status epilepticus: effect on neuronal damage, epileptogenesis, and behavioral alterations in rats. Neuropharmacology 51, 789–804. [PubMed: 16806297]

Brandt C, Potschka H, Loscher W, Ebert U, 2003 N-methyl-D-aspartate receptor blockade after status epilepticus protects against limbic brain damage but not against epilepsy in the kainate model of temporal lobe epilepsy. Neuroscience 118, 727–740. [PubMed: 12710980]

Bumanglag AV, Sloviter RS, 2008 Minimal latency to hippocampal epileptogenesis and clinical epilepsy after perforant pathway stimulation-induced status epilepticus in awake rats. The Journal of Comparative Neurology 510, 561–580. [PubMed: 18697194]

Chen Z, Brodie MJ, Liew D, Kwan P, 2018 Treatment outcomes in patients with newly diagnosed epilepsy treated with established and new antiepileptic drugs: a 30-year longitudinal cohort study. JAMA Neurol 75, 279–286. [PubMed: 29279892]

Clement JG, Hand BT, Shiloff JD, 1981 Differences in the toxicity of soman in various strains of mice. Fundamental and Applied Toxicology 1, 419–420. [PubMed: 7185592]

de Araujo Furtado M, Lumley LA, Robison C, Tong LC, Lichtenstein S, Yourick DL, 2010 Spontaneous recurrent seizures after status epilepticus induced by soman in Sprague-Dawley rats. Epilepsia 51, 1503–1510. [PubMed: 20067510]

Deshpande LS, DeLorenzo RJ, 2019 Novel therapeutics for treating organophosphate-induced status epilepticus co-morbidities, based on changes in calcium homeostasis. Neurobiology of Disease.

Doheny HC, Whittington MA, Jefferys JG, Patsalos PN, 2002 A comparison of the efficacy of carbamazepine and the novel anti-epileptic drug levetiracetam in the tetanus toxin model of focal complex partial epilepsy. British Journal of Pharmacology 135, 1425–1434. [PubMed: 11906955]

Dudek FE, Obenaus A, Schweitzer JS, Wuarin JP, 1994 Functional significance of hippocampal plasticity in epileptic brain: electrophysiological changes of the dentate granule cells associated with mossy fiber sprouting. Hippocampus 4, 259–265. [PubMed: 7842047]

Elmer E, Kokaia Z, Kokaia M, Lindvall O, McIntyre DC, 1997 Mossy fibre sprouting: evidence against a facilitatory role in epileptogenesis. Neuroreport 8, 1193–1196. [PubMed: 9175112]

Grabenstatter HL, Ferraro DJ, Williams PA, Chapman PL, Dudek FE, 2005 Use of chronic epilepsy models in antiepileptic drug discovery: the effect of topiramate on spontaneous motor seizures in rats with kainate-induced epilepsy. Epilepsia 46, 8–14.

Gu B, Dalton KA, 2017 Models and detection of spontaneous recurrent seizures in laboratory rodents. Zool Res 38, 171–179. [PubMed: 28825447]

Harvey BD, Sloviter RS, 2005 Hippocampal granule cell activity and c-Fos expression during spontaneous seizures in awake, chronically epileptic, pilocarpine-treated rats: implications for hippocampal epileptogenesis. The Journal of Comparative Neurology 488, 442–463. [PubMed: 15973680]

Itoh K, Inamine M, Oshima W, Kotani M, Chiba Y, Ueno M, Ishihara Y, 2015 Prevention of status epilepticus-induced brain edema and neuronal cell loss by repeated treatment with high-dose levetiracetam. Brain Research 1608, 225–234. [PubMed: 25770058]

Jung S, Jones TD, Lugo JN Jr., Sheerin AH, Miller JW, D'Ambrosio R, Anderson AE, Poolos NP, 2007 Progressive dendritic HCN channelopathy during epileptogenesis in the rat pilocarpine model of epilepsy. The Journal of Neuroscience 27, 13012–13021. [PubMed: 18032674]

Kim JE, Choi HC, Song HK, Jo SM, Kim DS, Choi SY, Kim YI, Kang TC, 2010 Levetiracetam inhibits interleukin-1 beta inflammatory responses in the hippocampus and piriform cortex of epileptic rats. Neuroscience Letters 471, 94–99. [PubMed: 20080147]

Klein P, Dingledine R, Aronica E, Bernard C, Blumcke I, Boison D, Brodie MJ, Brooks-Kayal AR, Engel J Jr., Forcelli PA, Hirsch LJ, Kaminski RM, Klitgaard H, Kobow K, Lowenstein DH, Pearl PL, Pitkanen A, Puhakka N, Rogawski MA, Schmidt D, Sillanpaa M, Sloviter RS, Steinhauser C, Vezzani A, Walker MC, Loscher W, 2018 Commonalities in epileptogenic processes from different acute brain insults: Do they translate? Epilepsia 59, 37–66. [PubMed: 29247482]

Klitgaard H, Matagne A, Gobert J, Wulfert E, 1998 Evidence for a unique profile of levetiracetam in rodent models of seizures and epilepsy. European Journal of Pharmacology 353, 191–206. [PubMed: 9726649]

Leite JP, Cavalheiro EA, 1995 Effects of conventional antiepileptic drugs in a model of spontaneous recurrent seizures in rats. Epilepsy Research 20, 93–104. [PubMed: 7750514]

Lemos T, Cavalheiro EA, 1995 Suppression of pilocarpine-induced status epilepticus and the late development of epilepsy in rats. Experimental Brain Research 102, 423–428. [PubMed: 7737389]

Longo BM, Mello LE, 1998 Supragranular mossy fiber sprouting is not necessary for spontaneous seizures in the intrahippocampal kainate model of epilepsy in the rat. Epilepsy Research 32, 172–182. [PubMed: 9761318]

Loscher W, 2007 The pharmacokinetics of antiepileptic drugs in rats: consequences for maintaining effective drug levels during prolonged drug administration in rat models of epilepsy. Epilepsia 48, 1245–1258. [PubMed: 17441999]

Loscher W, Honack D, 2000 Development of tolerance during chronic treatment of kindled rats with the novel antiepileptic drug levetiracetam. Epilepsia 41, 1499–1506. [PubMed: 11114206]

Marrero-Rosado B, de Araujo Furtado M, Schultz CR, Stone M, Kundrick E, Walker K, O'Brien S, Du F, Lumley LA, 2018 Soman-induced status epilepticus, epileptogenesis, and neuropathology in carboxylesterase knockout mice treated with midazolam. Epilepsia 59, 2206–2218. [PubMed: 30368799]

Matson LM, Lee-Stubbs RB, Cadieux CL, Koenig JA, Ardinger CE, Chandler J, Johnson EA, Hoard-Fruchey HM, Shih TA, Cerasoli DM, McDonough JH, 2018 Assessment of mouse strain differences in baseline esterase activities and toxic response to sarin. Toxicology 410, 10–15. [PubMed: 30172647]

McCarren HS, Arbutus JA, Ardinger C, Dunn EN, Jackson CE, McDonough JH, 2018 Dexmedetomidine stops benzodiazepine-refractory nerve agent-induced status epilepticus. Epilepsy Research 141, 1–12. [PubMed: 29414381]

McDonough JH Jr., Clark TR, Slone TW Jr., Zoeffel D, Brown K, Kim S, Smith CD, 1998 Neural lesions in the rat and their relationship to EEG delta activity following seizures induced by the nerve agent soman. Neurotoxicology 19, 381–391. [PubMed: 9621344]

McDonough JH Jr., Shih TM, 1997 Neuropharmacological mechanisms of nerve agent-induced seizure and neuropathology. Neuroscience and Biobehavioral Reviews 21, 559–579. [PubMed: 9353792]

McDonough JH Jr., Smith RF, Smith CD, 1986 Behavioral correlates of soman-induced neuropathology: deficits in DRL acquisition. Neurobehavioral Toxicology and Teratology 8, 179–187. [PubMed: 3713965]

Office of the Surgeon General, U.S.A., 2008 Medical Aspects of Chemical Warfare. Office of the Surgeon General, United States Army, Washington, DC.

Patsalos PN, Berry DJ, Bourgeois BF, Cloyd JC, Glauser TA, Johannessen SI, Leppik IE, Tomson T, Perucca E, 2008 Antiepileptic drugs--best practice guidelines for therapeutic drug monitoring: a position paper by the subcommission on therapeutic drug monitoring, ILAE Commission on Therapeutic Strategies. Epilepsia 49, 1239–1276. [PubMed: 18397299]

Shih TM, McDonough JH Jr., 1997 Neurochemical mechanisms in soman-induced seizures. Journal of Applied Toxicology 17, 255–264. [PubMed: 9285539]

Siso S, Hobson BA, Harvey DJ, Bruun DA, Rowland DJ, Garbow JR, Lein PJ, 2017 Spatiotemporal progression and remission of lesions in the rat brain following acute intoxication with diisopropylfluorophosphate. Toxicological Sciences 157(2), 330–341. [PubMed: 28329845]

Sloviter RS, 1987 Decreased hippocampal inhibition and a selective loss of interneurons in experimental epilepsy. Science 235, 73–76. [PubMed: 2879352]

Sloviter RS, 2008 Hippocampal epileptogenesis in animal models of mesial temporal lobe epilepsy with hippocampal sclerosis: the importance of the “latent period” and other concepts. Epilepsia 49 Suppl 9, 85–92. [PubMed: 19087122]

Sloviter RS, 2009 Experimental status epilepticus in animals: What are we modeling? Epilepsia 50 Suppl 12, 11–13.

Tauck DL, Nadler JV, 1985 Evidence of functional mossy fiber sprouting in hippocampal formation of kainic acid-treated rats. The Journal of Neuroscience 5, 1016–1022. [PubMed: 3981241]

Turski WA, Cavalheiro EA, Bortolotto ZA, Mello LM, Schwarz M, Turski L, 1984 Seizures produced by pilocarpine in mice: a behavioral, electroencephalographic and morphological analysis. Brain Research 321, 237–253. [PubMed: 6498517]

Turski WA, Cavalheiro EA, Coimbra C, da Penha Berzaghi M, Ikonomidou-Turski C, Turski L, 1987 Only certain antiepileptic drugs prevent seizures induced by pilocarpine. Brain Research 434, 281–305. [PubMed: 3607518]

United Nations Mission to Investigate Allegations of the Use of Chemical Weapons in the Syrian Arab Republic, 12 13, 2013 Final Report.

United Nations Security Council, 3 26, 1984 Report of the specialists appointed by the Secretary-General to investigate allegations by the Islamic Republic of Iran concerning the use of chemical weapons.

van Vliet EA, Edelbroek PM, Gorter JA, 2010 Improved seizure control by alternating therapy of levetiracetam and valproate in epileptic rats. Epilepsia 51, 362–370. [PubMed: 19674045]

van Vliet EA, van Schaik R, Edelbroek PM, da Silva FH, Wadman WJ, Gorter JA, 2008 Development of tolerance to levetiracetam in rats with chronic epilepsy. Epilepsia 49, 1151–1159. [PubMed: 18266746]

Vossler DGW. M; Gidal BE, 2018 Summary of Antiepileptic Drugs Available in the United States of America, in: Society, A.E (Ed.), CURRENT REVIEW IN CLINICAL SCIENCE.

Wehner JM, Murphy-Erdosh C, Smolen A, Smolen TN, 1987 Genetic variation in paraoxonase activity and sensitivity to diisopropylphosphofluoridate in inbred mice. Pharmacology, Biochemistry, and Behavior 28, 317–320.

Williams PA, White AM, Clark S, Ferraro DJ, Swiercz W, Staley KJ, Dudek FE, 2009 Development of spontaneous recurrent seizures after kainate-induced status epilepticus. The Journal of neuroscience : the official journal of the Society for Neuroscience 29, 2103–2112. [PubMed: 19228963]

Yanagisawa N, Morita H, Nakajima T, 2006 Sarin experiences in Japan: acute toxicity and long-term effects. Journal of the Neurological Sciences 249, 76–85. [PubMed: 16962140]

Highlights

- Soman-induced SE led to recurrent seizures in all mice with minimal latency
- Seizure burden varied considerably between mice
- Lesions were restricted to the amygdala, piriform cortex, and CA1
- Levetiracetam modified seizure characteristics, but did not lower seizure burden
- Phenobarbital delayed onset of seizures, while valproic acid was ineffective

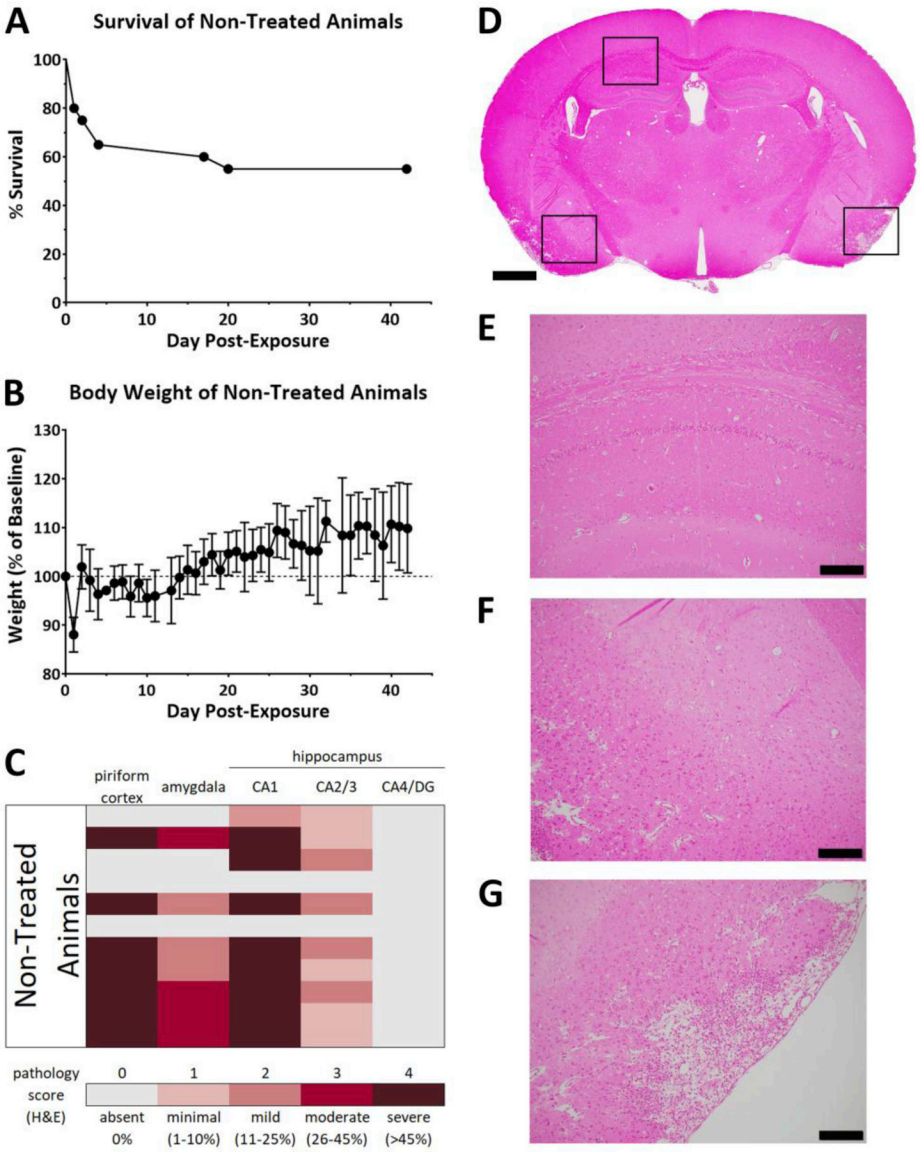

Figure 1: Long-term effects of soman exposure in mice that were not treated with AEDs.

(A) Survival among mice that were not treated with any antiepileptic drugs or vehicles decreased rapidly over the first 4 d after nerve agent exposure, but subsequently remained stable over 28 d. (B) Body weight of non-treated mice returned to baseline within 2 d after nerve agent exposure. (C) The majority of untreated mice displayed neuropathology, with the most severe damage occurring in the piriform cortex and CA1, and moderate damage to the amygdala. Each row represents scores from a single mouse. (D-G) Representative H&E staining in an untreated mouse. Boxes in (D) show locations of higher-resolution images of CA1 (E), amygdala (F), and piriform cortex (G). These areas display a large number of dead cells and tissue loss. Scale bar is 1 mm (D) and 100 μ m (E-G).

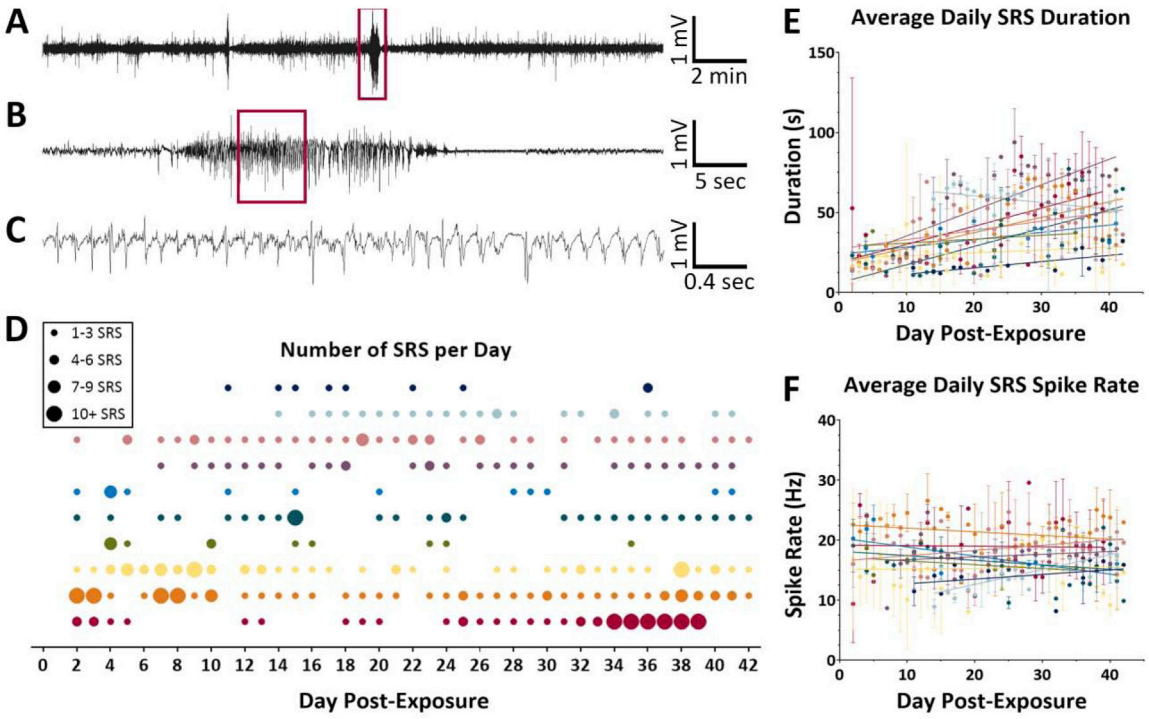

Figure 2: Emergence of SRS activity in mice that were not treated with AEDs.

(A) Representative cortical EEG trace demonstrating a spontaneous recurrent seizure (SRS) event, boxed in red. (B) Higher-magnification view of the SRS in panel A illustrating seizure onset, progression, post-ictal amplitude reduction, and return to baseline activity. (C) Higher-magnification view of the section of the SRS boxed panel B illustrating spike morphology. (D) The number of SRS per day is depicted by bubble size, with each mouse presented in a different color. (E-F) Daily average spike rate (E) and SRS duration (F) for each mouse. The slope of the best-fit line was used to determine changes over the course of the study. Individual animals are represented by the same color in panels D, E, and F.

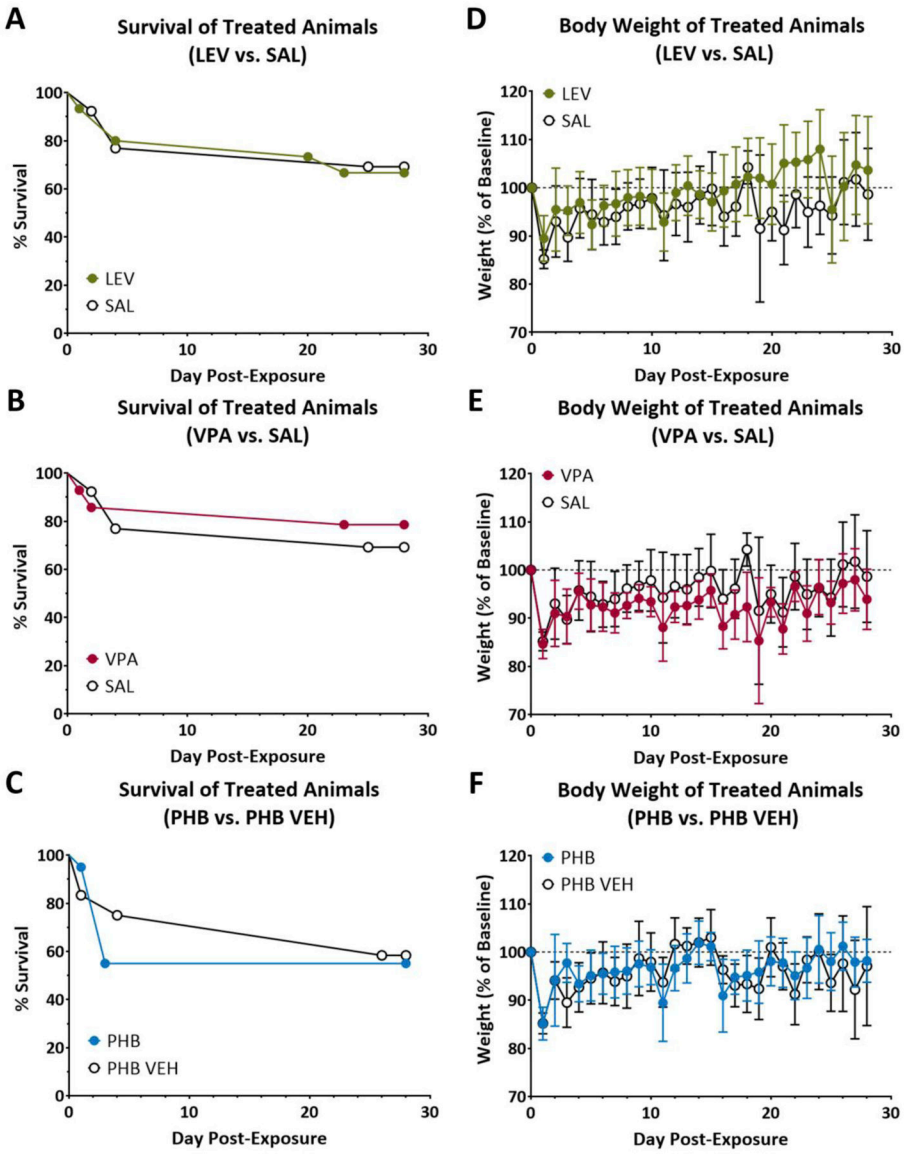

Figure 3: Physiological outcomes in mice treated with AEDs.

(A-C) Survival curves for mice treated with LEV (A), VPA (B), or PHB (C) did not differ from those of vehicle-treated mice. (D-F) Body weights for mice treated with LEV (D), PHB (F), and SAL (D,F) returned to baseline within a similar time frame to animals in the model characterization phase of the study, while those treated with VPA (E) or PHB VEH (F) recovered more slowly. Because the same SAL controls were used for both LEV and VPA, SAL data are plotted in panels A, B, D, and E to facilitate visual comparisons of each drug with their shared control.

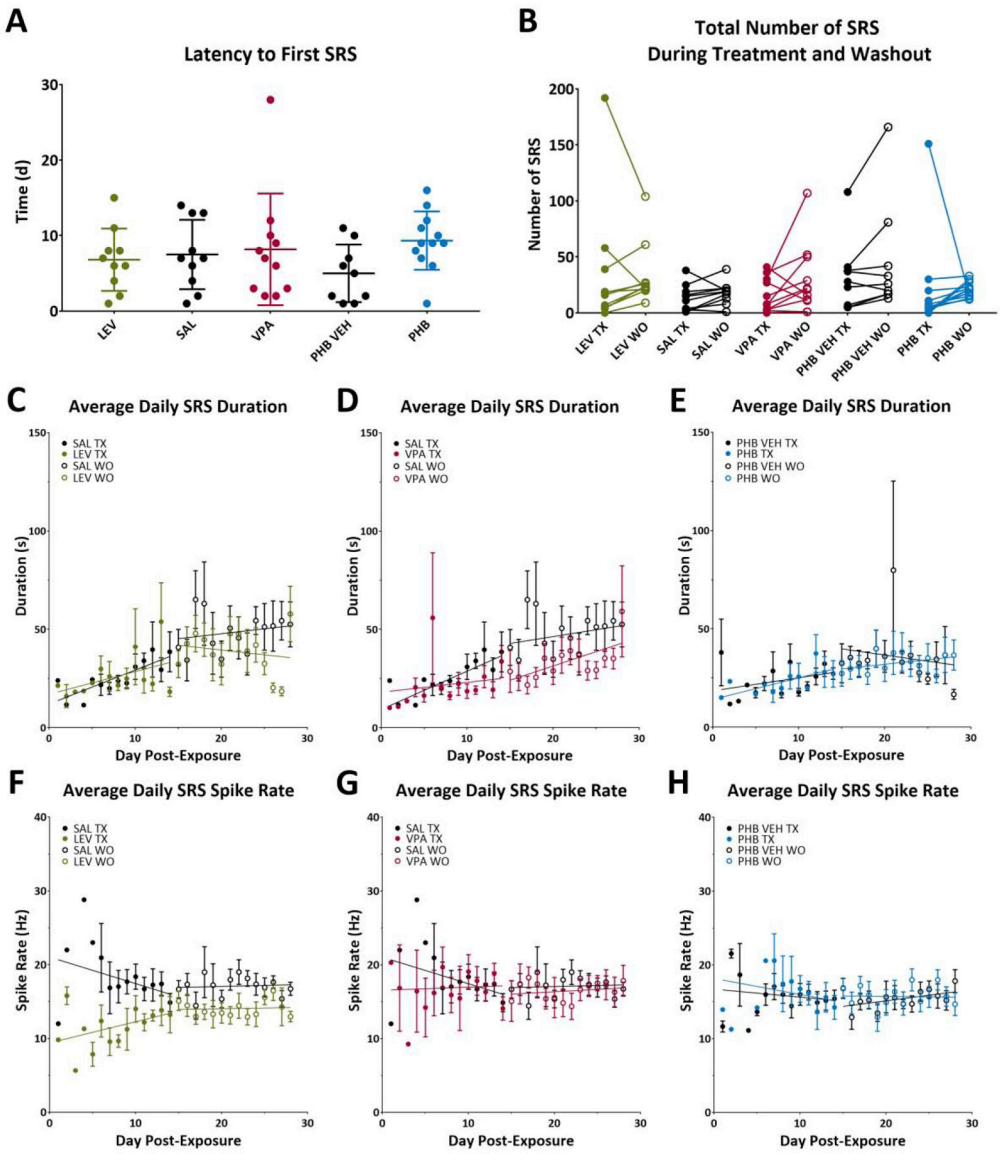

Figure 4: Effects of AEDs on SRS in soman-exposed mice.

(A) The latency to first spontaneous recurrent seizure (SRS) did not differ between LEV or VPA and their SAL control group, whereas PHB treatment led to significantly delayed onset of SRS compared to the PHB VEH group. (B) The total number of SRS experienced by each treatment group during the 14 d treatment period (TX) versus the 14 d washout period (WO) did not differ, nor was there an effect of treatment versus the appropriate control. (C-E) Average daily duration of SRS for mice treated with LEV (C), VPA (D), PHB (E), or corresponding controls. (F-H) Average spike rates LEV (F), VPA (G), PHB (H), or corresponding controls. For C-H, the slope and intercept of the best-fit lines for treatment and washout periods were used to determine whether each metric was affected by drug versus vehicle and TX versus WO.

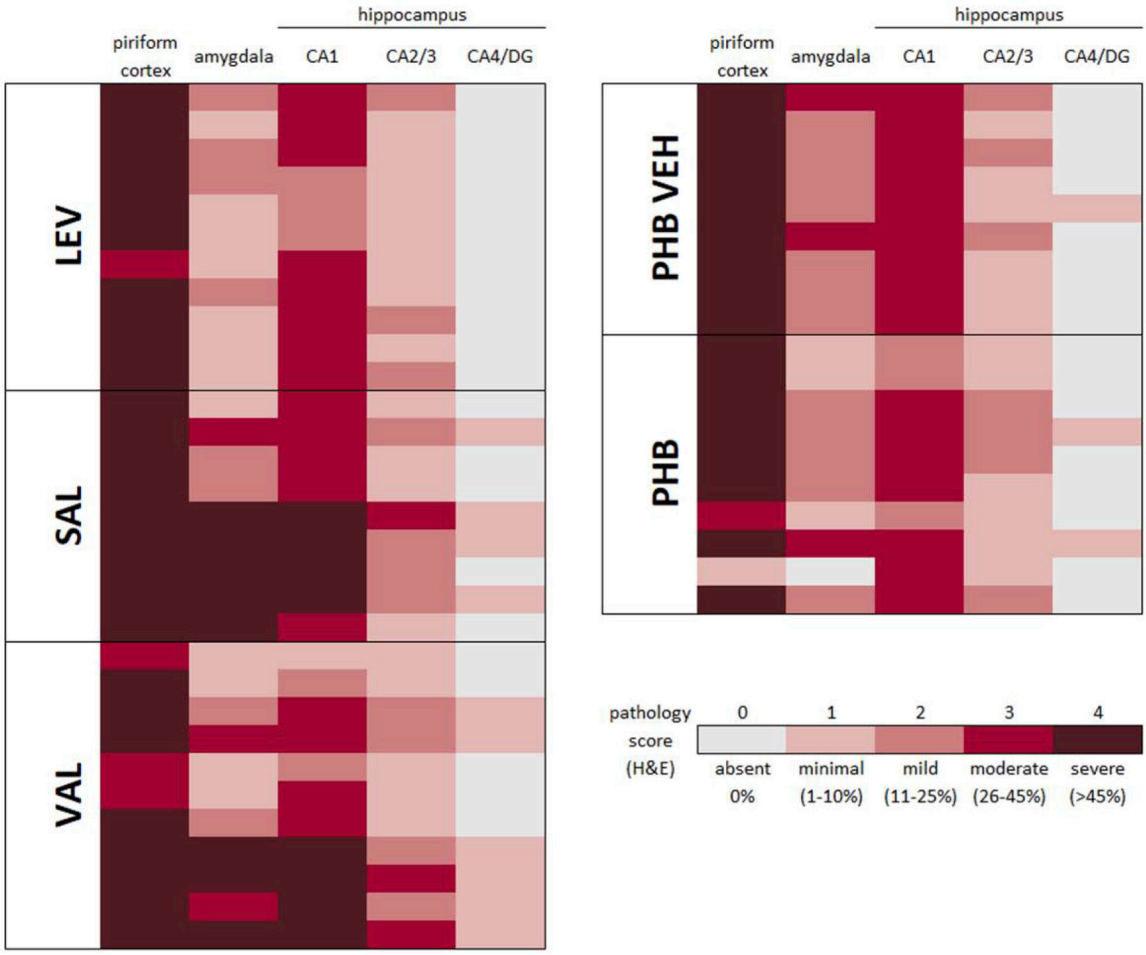

Figure 5: Effects of AEDs on histopathological lesions in soman-exposed mice.

Mice treated with LEV had reduced neuropathology scores in the amygdala, CA1, and CA4/dentate gyrus (DG) relative to SAL controls. Histopathology scores of mice treated with VPA did not differ from SAL in any brain region examined, nor were differences observed between the PHB and PHB VEH groups.